Original Article

Design, Synthesis and Biological Evaluation of Novel Piperidinyl Chalcones

Aravinda Pai, B.S. Jayashree*

Department of Pharmaceutical Chemistry, Manipal College of Pharmaceutical Sciences, Manipal Academy of Higher Education, Manipal, Karnataka, INDIA.

ABSTRACT

Aim/Background: Chalcones are one of the important class of compounds possessing a wide range of biological properties [Dinmock 1999, Go 2005]. One of the extensive area in research on chalcones is expressed in terms of their ability to act on various cancer cell lines by a variety of molecular mechanisms. Chalcones possessing methoxy groups, a trimethoxy substituted chalcone (PGHSD 234) is the most potent chalcone with cytotoxicity comparable to the standard drugs. **Materials and Methods:** The anti-oxidant potential in terms of their free radical scavenging ability and antiproliferative activities were evaluated. Log *P* value and cyclic Voltammetric studies were carried out to assess their hydrophobicity and to determine their anti-oxidant potential. MTT (methyl tetrazolium) assay was performed on two cell lines including Vero and MCF-7 cell lines. Molecular docking studies were performed to assess the binding pattern of synthesized chalcones into the ATP binding site of CDK2/Cyclin A protein target. **Results:** The MTT assay results showed the effect of various substituents on the chalcone template that could influence their cytotoxic effect. The hydrophobicity of the synthesized compounds were reported as distribution coefficient (Log D) and all the compounds showed Log D values in the range of 1.45–4.0. The cyclic voltammetric studies revealed their irreversible oxidation potential and were found in the range of -0.400 to -0.654. **Conclusion:** The present study provides insight for the better understanding of mechanistic studies of N-methyl piperidinyl chalcones against anticancer targets such as CDK and aromatase identified in breast cancer.

Key words: Chalcones, Piperidinyl, Cancer, CDK2/Cyclin A, Docking.

INTRODUCTION

Chalcones are one of the important class of compounds possessing a wide range of biological properties [Dinmock 1999, Go 2005]. One of the extensive area in research on chalcones is expressed in terms of their ability to act on various cancer cell lines by a variety of molecular mechanisms.[1] They exert anticancer activity by several mechanisms including inhibition of angiogenesis, interfering with p53 pathways,[2] inducing mitochondrial uncoupling and also act at different phases of cell cycle.[3,4] Chalcones have unique structural feature, which is responsible for its antimitotic activity. The unsaturated enone moiety present in chalcones can directly interact with the thiol (-SH) residue at the substrate binding pocket of tubulin where, it competes for the colchicine binding site resulting in the disruption of tubulin polymerization and inhibition of mitosis.[5,6] Extensive literature search provided the information on methoxylated chalcones and their role in the inhibition of mitosis which can be further correlated to the structures of antimitotic agents like Combrestatin A and colchicine having number of methoxy substituents. Chalcones possessing methoxy groups, a trimethoxy substituted chalcone (PGHSD 234) is the most potent chalcone with cytotoxicity comparable to the standard drugs. It has a percentage inhibition value of 0.21nM showing cytotoxicity against K562 lymphocytic leukemia cells and also

Submission Date: 27-12-2018;
Revision Date: 29-03-2019;
Accepted Date: 26-06-2019

DOI: 10.5530/ijper.53.3s.101

Correspondence:
Dr. B.S. Jayashree,
Professor, Department of Pharmaceutical chemistry, Manipal College of Pharmaceutical Sciences, Manipal Academy of Higher Education (MAHE), Manipal-576 104, Karnataka, INDIA.
Phone: +91 98459 95895
E-mail: jayashree.sy@gmail.com

www.ijper.org

a good disruptor of microtubule assembly with a percentage inhibition value of 0.5 μM. It is noteworthy to mention the importance of methoxy group in chalcones, for instance, the increase in the number of methoxy groups could drastically increase the lipophilicity and thus reduces their water solubility and drug-likeliness. One of the crucial approaches used to manipulate the lipophilicity induced by methoxy groups is to, acquaint the chalcone template with hydrophilic substituents. The substitution with basic aliphatic amino entity, that are easily protonated at the physiological pH, is an intelligent approach. In the present investigation, the synthesis of a novel series of methoxy substituted chalcones substituted with a basic N-methylpiperidinyl group on the ring was undertaken. The introduction of N-Methyl piperidinyl substitution has a prominent effect on the physicochemical characteristics of the test compounds. It is (pKa 10) protonated at physiological pH, which could enhance its aqueous solubility. The basic characteristics of the piperidine ring is solely responsible for many types of interactions, one of them being hydrogen bonding interactions at the active sites of many targets. Interestingly, many of the research groups have reported enhanced selectivity as well as potency in such systems.

MATERIALS AND METHODS

Molecular docking studies

The docking study was performed with maestro molecular modeling platform (version 10.5) available with Schrödinger, LLC.

Step wise docking protocol

Protein Preparation

The ligand bound three-dimensional X-ray structure was obtained from the Protein Data Bank [PDB] ID: 4 FX3)[7] with high resolution. The protein preparation was done by protein preparation wizard application. It includes steps such as preparation as well as refinement.

Ligand Preparation

The ligand preparation was done using ligprep tool.[8] The force field OPLS 2005 was used for this purpose. The ionization states were generated using the application EPIK. In this study, a series of 10 N- methyl piperidinyl substituted chalcone derivatives were employed for the docking process.

Ligand Alignment

For assuring better docking poses, flexible ligand alignment was carried out.

Extra precision Glide™ Docking

GLIDE docking protocol involves two steps. In the first step, a GRID is generated and in the second step the designed ligands are docked into the active site and are scores according to their binding free energy. The XP GLIDE uses a specific algorithm, which semi quantitatively ranks the ligands by their ability to bind to a specific conformation of a protein receptor. The rigid receptor approximation used in GLIDE enable us to find out ligands with maximum steric clashes, which otherwise bind to a different conformation of the same receptor. The interaction of crystal ligand at the active site of CDK2/Cyclin A is shown in Figure 1. Figure 2 showed the 2D interaction of the crystal ligand at the active site of CDK2/Cyclin A. The electrostatic potential surface of crystal ligand is shown in Figure 3. The interaction of most active analogue NMC5 at the active site of CDK2/Cyclin A is presented in Figure 4 also, the 2D interaction of NMC5 is shown in Figure 5. Figure 6 represents the electrostatic potential binding surface of most active analogue NMC5. The interaction of standard drug flavopiridol at the active site of CDK2/Cyclin A is given in Figure 7 and also, its 2D

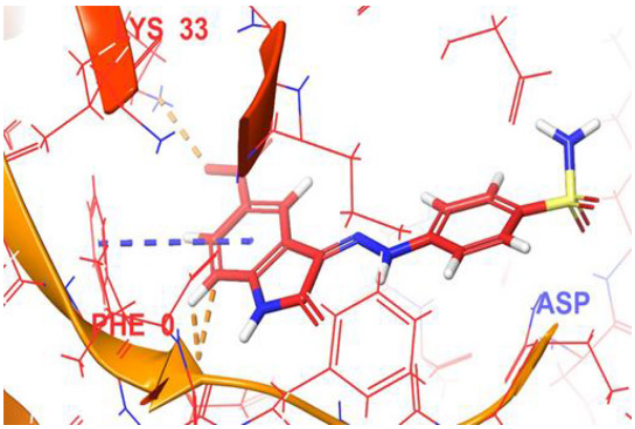

Figure 1: Interaction of crystal ligand at the active site of CDK2/Cyclin A.

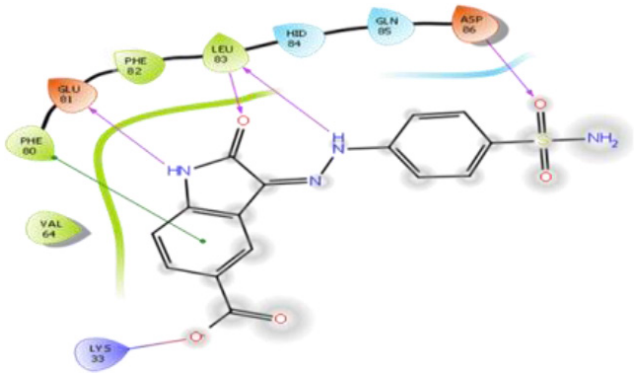

Figure 2: 2D interaction of crystal ligand at the active site of CDK2/Cyclin A.

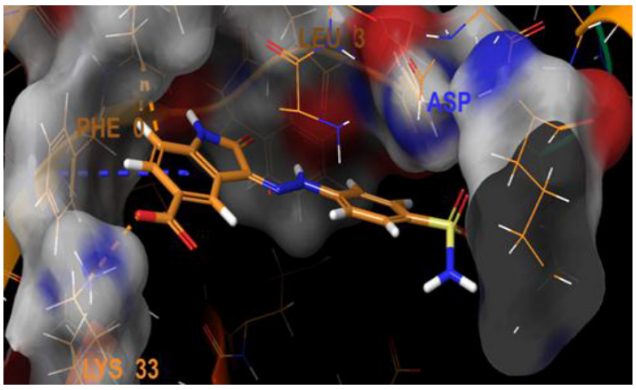

Figure 3: Electrostatic potential surface of crystal ligand.

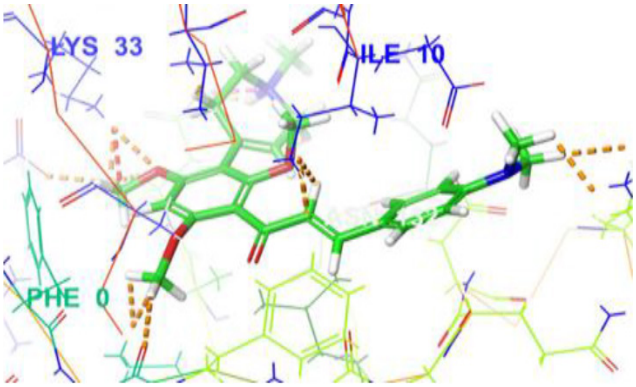

Figure 4: Interactions of the most active analogue NMC5 at the active site of CDK2/Cyclin A.

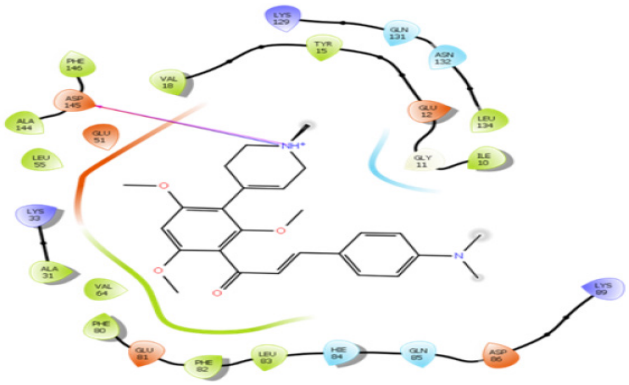

Figure 5: 2D Interactions of the most active analogue NMC5 at the active site of CDK2/Cyclin A.

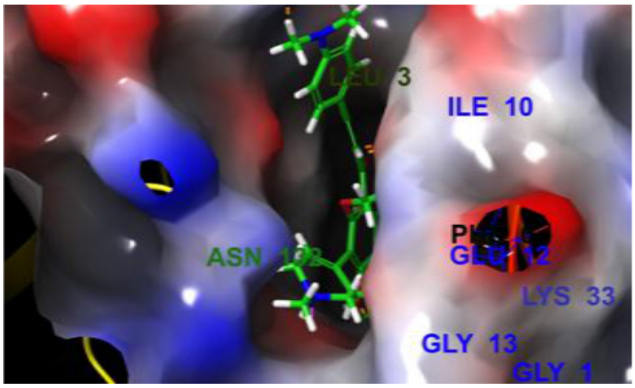

Figure 6: Electrostatic potential binding surface of NMC5.

interaction is represented in Figure 8. The electrostatic potential binding surface of flavopiridol is presented in Figure 9. Table 1 provides the docking scores of all the test compounds.

Major Glide XP scoring functions

Displacement of waters from the protein cavity by hydrophobic ligands

The ability of lipophilic ligands to displace water molecules from the hydrophobic sites on the receptor protein: Displacement of water molecules from the binding cavity into the bulk is an energetically favourable process. The stagnant water molecules will decrease the entropy of the system whereby, they drastically increase the binding free energy. Suitably designed lipophilic ligands will displace water molecules from the binding surface into the bulk and are positive contributors for the entropy.

Protein-ligand hydrogen bonding interactions as well as other type of columbic interactions

The quality and types of hydrogen bonding that takes place between the ligand and active site residues has a large impact on binding affinity. Other type of interactions

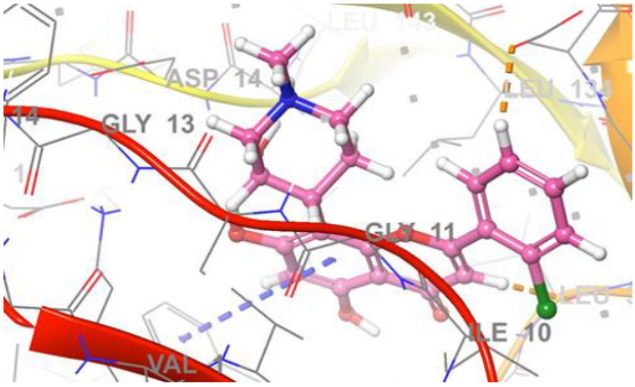

Figure 7: Interactions of Flavopiridol at the active site of CDK2/Cyclin A.

includes, electrostatic interactions also contribute largely to the binding affinity.

Desolation effects

Polar or charged groups of either ligand or the residues, were formerly solvent exposed were desolated resulting in either partial or total loss of their ability to make hydrogen bonds. The final outcome was a decrease in binding affinity.

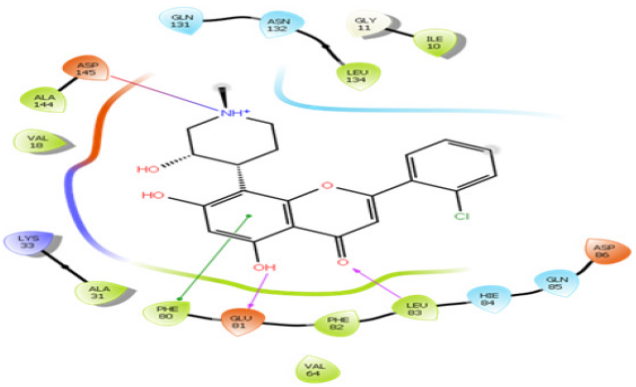

Figure 8: 2D Interactions of Flavopiridol at the active site of CDK2/Cyclin A.

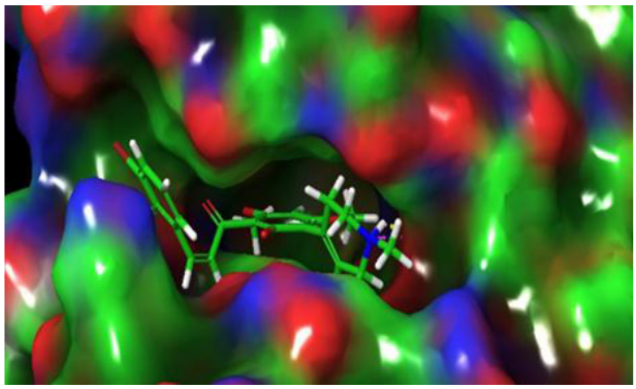

Figure 9: Electrostatic potential binding surface of Flavopiridol.

Table 1: Docking scores of reference and synthesized compounds.

Compounds	docking score	glide ligand efficiency	glide ligand efficiency sa
Crys. Lig	−12.812	−0.205	−0.651
Flavopiridol	−9.576	−0.198	−0.627
NMC5	−9.369	−0.202	−0.622
NMC9	−8.588	−0.202	−0.622
NMC6	−8.159	−0.214	−0.642
NMC7	−7.921	−0.195	−0.585
NMC3	−7.184	−0.167	−0.526
NMC4	−7.173	−0.181	−0.549
NMC10	−6.93	−0.171	−0.526
NMC1	−6.862	−0.164	−0.51
NMC2	−6.702	−0.165	−0.508
NMC8	−6.559	−0.004	−0.013

Entropic effects due to the steric restriction of either the protein or the ligand groups

Partial or total restriction of rotational or vibrational motion of either the ligand group or the interactive protein residue will have direct effects on the entropy and thereby, decrease the binding affinity.

Metal ligand interactions

Ligand interacting with a metal ion will have positive effect on binding affinity.

Generally, a large number of empirical functions have been derived for the assessment of binding affinity between a ligand and a protein target. One of the highly utilised functions is Chem Score. Chem score contains a hydrophobic atom- atom pair energy term represented in the form of:

$$E_{phobic\_pair} = \sum_{ij} f(rij)$$

Here i and j refer to the lipophilic atoms and rij refers to the interatomic distance between the two atoms. Chem score evaluates the protein ligand interactions based on the geometric criteria. It does not consider desolvating effects. It also uses simple rotational bond term to calculate the entropy arising due to the restricted rotation.

Extra precision docking rewards and penalties

Reward for hydrophobic enclosure reward

Planar aromatic rings are enclosed between the hydrophobic protein residues would contribute positively to the binding affinity. The hydrophobic enclosure reward for the crystal ligand, flavopiridol and active analogue NMC5 is given in Figures 10, 12 and 14 respectively.

Reward for the hydrophobically packed hydrogen bonds

Ligand groups forming hydrogen bonding interactions with the hydrophobic groups of protein in the Hinge region will get a reward of 3-4 KJ/Mole. Whereas, reward for hydrophobically packed hydrogen bonds are presented in the Figure 11 and 13 respectively.

Electrostatic rewards

This could happen in one of the several circumstances. Ligand groups with charges engrossed in the low electrostatic potential environments.

Existence of Zwitterionic configurations increases the total electrostatic attraction.

When positive group of the ligand binds to a weekly solvated negative group of protein.

Extra precision docking penalties

Rotational penalties: This could arise because of a large number of rotatable bonds in ligand groups.

Solvent exposure penalties: Large groups present in ligands will receive solvent exposure penalty.

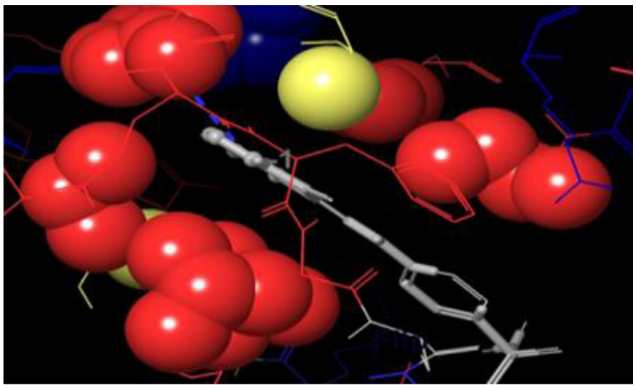

Figure 10: Crystal ligand hydrophobic enclosure reward.

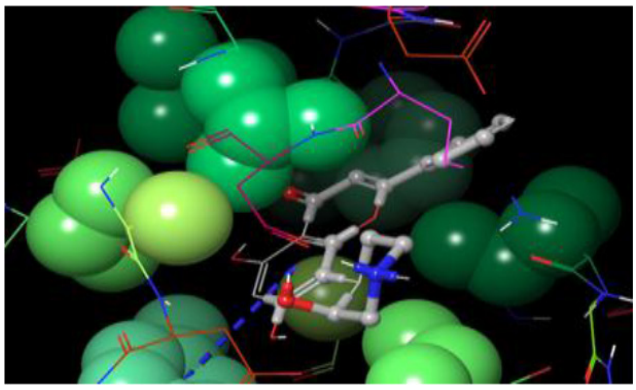

Figure 12: Flavopiridol hydrophobic enclosure reward.

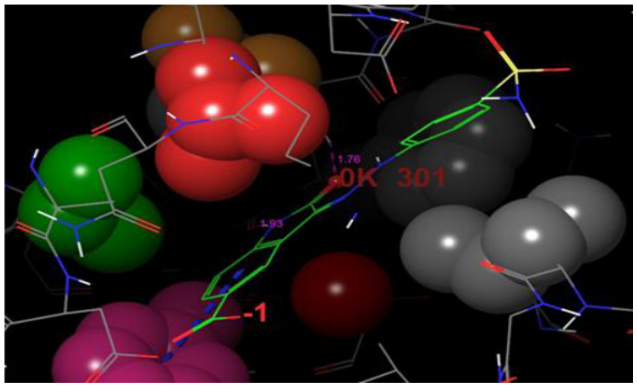

Figure 11: Crystal ligand hydrophobically packed hydrogen bonds.

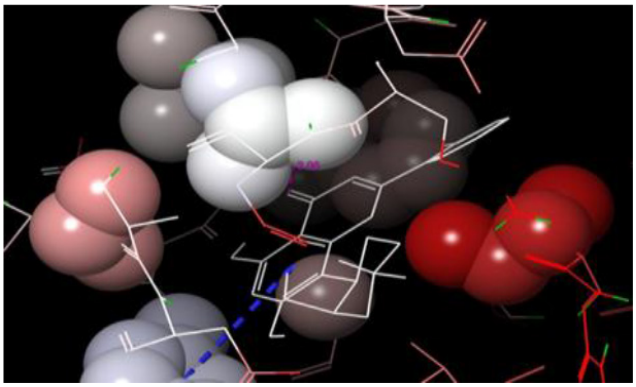

Figure 13: Flavopiridol hydrophobically packed hydrogen bonds.

Validation of Docking Process

The RMSD (root mean square deviation) parameter was used to assess the accuracy of the docking protocol. The RMSD in this case was found to be 0.3 and was found well within the limit of 2.

Chemistry

Instruments, chemicals and reagents

All the chemicals and regents were purchased from Sigma chemicals, SRL Ranbaxy and Cisco chemicals. Redox potential was recorded using CH-electrochemical analyzer USA, UV spectrum was recorded using Shimadzu UV-1800, IR spectrum was recorded using IR affinity from Shimadzu and Mass spectrum was recorded using LCMS utilizing APCI as ionization method, NMR spectrum was recorded using Bruker-400.

Synthesis

Preparation of Step I

1-Methyl-4-(2,4,6-trimethoxyphenyl)-1,2,3,6-tetrahydropyridine(2):methyl substituted piperidone (0.01 molar) was stirred with a solution of 1,3,5-trimethoxybenzene (0.15 mol) in an anhydrous glacial acetic acid (100 ml) solvent on an ice bath maintained at 5°C. Further, hydrochloric acid (10ml) was slowly added to the reaction mixture for about 1 h and later the reaction mixture was stirred for 24 h at 25°C. It was then heated at the temperature of 90-100°C for about 3 h.[9] The solvent was removed using Rota evaporator and further diluted with distilled water. The aqueous solution was then basified using 1 molar sodium hydroxide and the product was filtered, dried and recrystallized with a mixture of acetone and water. The compound was characterized by spectrochemical methods. The mechanism of selective demethylation using BF3 is given in Figure 15.

Preparation of Step II

The product of Step I (2) is reacted with Boron trifluride dimethyl etherate (3 ml, 0.005 molar) in CH_2Cl_2 (50 ml), the freezing temperature was maintained for 4 h. After the completion of 4 h, the reaction mixture was treated with acetic anhydride (3 ml) and the reaction mixture was further stirred for 24 h. It was then diluted with distilled water and the compound was precipitated using sodium carbonate (3). The product was then recrystal-

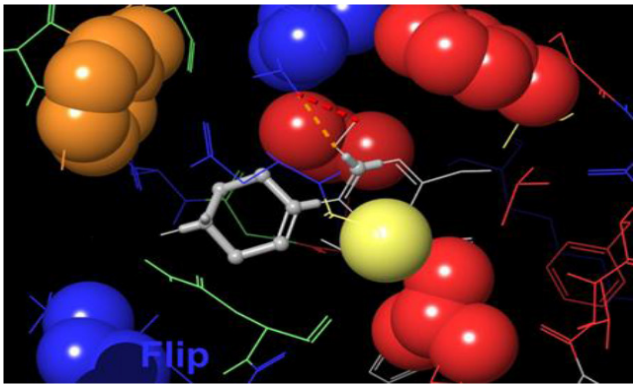

Figure 14: NMC5 hydrophobic enclosure reward.

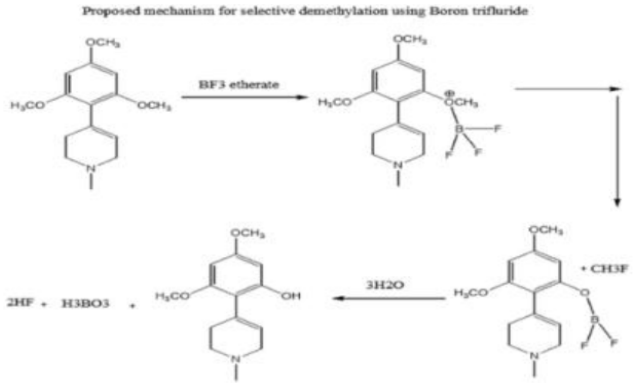

Figure 15: Schematic representation of selective DE- methylation mechanism using BF_3.

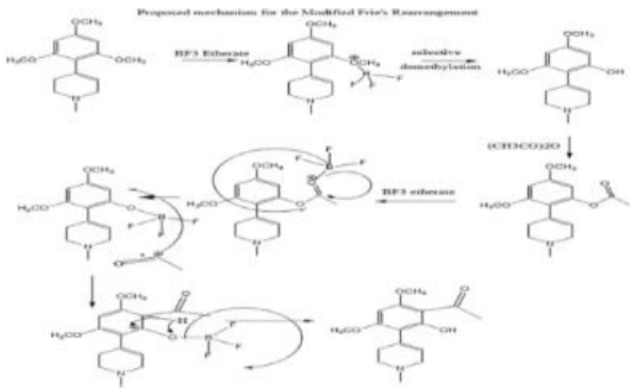

Figure 16: Schematic representation of modified Frie's rearrangement mechanism.

lized using a mixture of acetone and water. The product was further characterized.

A novel mechanism was proposed for the regioselective demethylation employing Boron trifluride etherate complex. BF3 complexes with one of the methoxy groups and forms an ion pair like intermediate, which then loses one fluoride ion and combines with methyl group to give methyl fluride. In the next step, the complex is hydrolyzed with water to give a demethylated product, boric acid and hydrogen fluoride.

A mechanism was later proposed for the ortho acylation of the demethylated product. The reaction proceeds like a classical Frie's rearrangement reaction, where, boron trifluride was used instead of anhydrous aluminum chloride, thus the reaction becomes a modification of the Frie's reaction. The present reaction is named as modified Frie's rearrangement. The mechanism of modified Frie's rearrangement reaction is given in Figure 16.

Preparation of chalcones

Chalcones were synthesized using standard methods employing Claisen Schmidt reaction. An equimolar mixture of 3 and corresponding aldehydes were added to the alcoholic solution of potassium hydroxide and stirred for 14 h. The reaction progress was monitored by TLC using the solvent system Chloroform: methanol in the ratio of (9:1). The reaction mixture was added to the ice, filtered and recrystallized using methanol water mixture. The scheme for the synthesis of final compounds were presented in Figure 17.

(2E)-1-(3-(1,2,3,6-tetrahydro-1-methylpyridin-4-yl)-2-hydroxy-4,6-dimethoxyphenyl)-3-(1H-indol-3-yl) prop-2-en-1-one (JAPC1) $C_{25}H_{26}N_2O_4$, Yellow crystalline, Molecular weight 418.25, UV: λ_{max} 353.5 nm (ɛmax 38000), FT-IR ʋ´max (cm^{-1}): 1631 (C=O); Mass (APCI + ve mode): m/z 418.19 $[M+1]^+$ (100%) ^1H NMR: δ 2.28-2.40 (5H, 2.28 (s), 2.34 (ddd, *J* = 15.0, 3.8, 2.0 Hz)), 2.72 (2H, ddd, *J* = 11.4, 3.8, 2.0 Hz), 3.08 (2H, dd, *J* = 13.9, 2.2 Hz), 3.85-3.86 (6H, 3.86 (s), 3.86 (s)), 5.98 (1H, dd, *J* = 4.3, 2.2 Hz), 6.12 (1H, s), 6.66 (1H, d, *J* = 15.6 Hz), 7.08 (1H, ddd, *J* = 8.0, 7.8, 1.6 Hz), 7.19 (1H, ddd, *J* = 8.0, 7.8, 1.5 Hz), 7.50 (1H, ddt, *J* = 8.0, 1.6, 0.5 Hz), 7.58-7.67 (2H, 7.63 (t, *J* = 0.4 Hz), 7.62 (d, *J* = 15.6 Hz)), 7.85 (1H, ddt, *J* = 8.0, 1.5, 0.4 Hz).

(2E)-1-(3-(1,2,3,6-tetrahydro-1-methylpyridin-4-yl)-2-hydroxy-4,6-dimethoxyphenyl)-3-phenyl-prop-2-en-1-one(JAPC2) $C_{23}H_{25}NO_4$, Light yellow crystalline, Molecular weight 378.2 UV: λ_{max} 343 nm (ɛmax 43000), FT-IR ʋ´max (cm^{-1}): 1631 (C=O), Mass (APCI + ve mode) :m/z 379.18 $[M+1]^+$ (100%) ^1H NMR: δ 2.28-2.40 (5H, 2.28 (s), 2.34 (ddd, *J* = 15.0, 3.8, 2.0 Hz)), 2.72 (2H, ddd, *J* = 11.4, 10.1, 3.8 Hz), 3.08 (2H, dd, *J* = 13.9, 4.3 Hz), 3.85-3.86 (6H, 3.86 (s), 3.86 (s)), 5.98 (1H, dd, *J* = 4.3, 2.2 Hz), 6.12 (1H, s), 6.72 (1H, d, *J* = 15.6 Hz), 7.38-7.50 (4H, 7.43 (tt, *J* = 7.5, 1.3 Hz), 7.45 (d, *J* = 15.6 Hz), 7.43 (dddd, *J* = 8.1, 7.5, 2.0, 0.5 Hz)), 7.50 (2H, dddd, *J* = 8.1, 2.3, 1.3, 0.5 Hz).

(2E)-1-(3-(1,2,3,6-tetrahydro-1-methylpyridin-4-yl)-2-hydroxy-4,6-dimethoxyphenyl)-3-(4-methoxy-

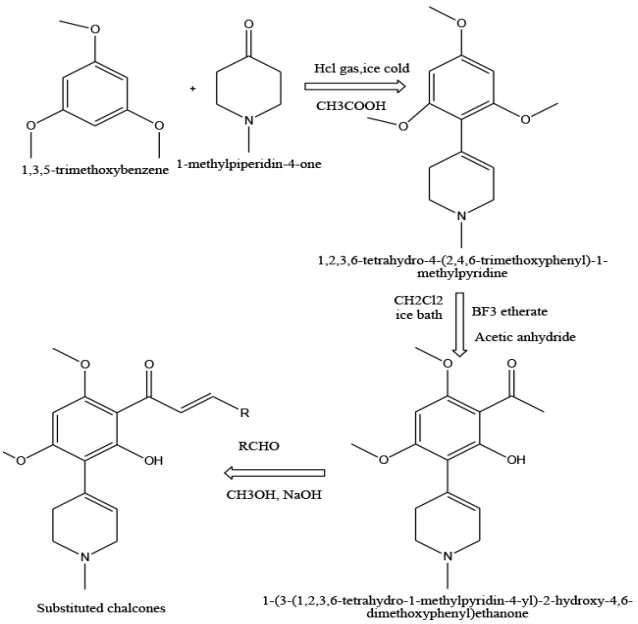

Figure 17: Scheme for the synthesis of title compounds.

phenyl)prop-2-en-1-one (JAPC3) $C_{24}H_{27}NO_5$, Brown crystalline, Molecular weight 409.09, UV: λ_{max} 358 nm (ε_{max} 58000), FT-IR υ'_{max} (cm^{-1}): 1631 (C=O) Mass (APCI +ve mode): m/z 410.19$[M+1]^+$ ^1H NMR: δ 2.28-2.40 (5H, 2.28 (s), 2.34 (ddd, *J* = 15.0, 3.8, 2.0 Hz)), 2.72 (2H, ddd, *J* = 11.4, 10.1, 3.8 Hz), 3.08 (2H, dd, *J* = 13.9, 4.3 Hz), 3.77 (3H, s), 3.85-3.86 (6H, 3.85 (s), 3.86 (s)), 5.98 (1H, dd, *J* = 4.3, 2.2 Hz), 6.19 (1H, s), 6.62 (1H, d, *J* = 15.6 Hz), 7.20 (2H, ddd, *J* = 8.8, 1.2, 0.5 Hz), 7.38 (1H, d, *J* = 15.6 Hz), 7.47 (2H, ddd, *J* = 8.8, 1.8, 0.5 Hz).

(2E)-1-(3-(1,2,3,6-tetrahydro-1-methylpyridin-4-yl)-2-hydroxy-4,6-dimethoxyphenyl)-3-(2-hydroxyphenyl)prop-2-en-1-one (JAPC4) $C_{23}H_{25}NO_5$, yellow crystalline, Molecular weight 386.12, UV: λ_{max} 336 nm (ε_{max} 23000), FT-IR υ'_{max} (cm^{-1}): 1631 (C=O) Mass (APCI +ve mode): m/z 396.18$[M+1]^+$ ^1H NMR: δ 2.28-2.40 (5H, 2.28 (s), 2.34 (ddd, *J* = 15.0, 3.8, 2.0 Hz)), 2.72 (2H, ddd, *J* = 11.4, 3.8, 2.0 Hz), 3.08 (2H, dd, *J* = 13.9, 4.3 Hz), 3.85-3.86 (6H, 3.85 (s), 3.86 (s)), 5.98 (1H, dd, *J* = 4.3, 2.2 Hz), 6.19 (1H, s), 6.65 (1H, d, *J* = 15.6 Hz), 6.89 (1H, ddd, *J* = 8.0, 1.1, 0.5 Hz), 7.18 (1H, ddd, *J* = 7.7, 7.5, 1.1 Hz), 7.31-7.43 (2H, 7.38 (ddd, *J* = 8.0, 7.5, 1.4 Hz), 7.35 (d, *J* = 15.6 Hz)), 7.69 (1H, ddd, *J* = 7.7, 1.4, 0.5 Hz).

(2E)-3-(2-bromophenyl)-1-(3-(1,2,3,6-tetrahydro-1-methylpyridin-4-yl)-2-hydroxy-4,6-dimethoxyphenyl)prop-2-en-1-one (JAPC5) $C_{23}H_{24}BrNO_4$, Yellow crystalline, Molecular weight 458.34, UV: λmax 368 nm (ε_{max} 67000), FT-IR υ'_{max} (cm^{-1}): 1631 (C=O) Mass (APCI +ve mode): m/z 459.09, $[M+1]^+$ ^1H NMR: δ 2.27-2.42 (5H, 2.28 (s), 2.34 (ddd, *J* = 15.0, 10.1, 3.8 Hz)), 2.72 (2H, ddd, *J* = 11.4, 10.1, 3.8 Hz), 3.08 (2H, dd, *J* = 13.9, 4.3 Hz), 3.85-3.86 (6H, 3.85 (s), 3.86 (s)), 5.98 (1H, dd, *J* = 4.3, 2.2 Hz), 6.20 (1H, s), 6.67 (1H, d, *J* = 15.7 Hz), 7.26 (1H, ddd, *J* = 7.8, 7.3, 1.6 Hz), 7.43-7.54 (3H, 7.49 (d, *J* = 15.7 Hz), 7.47 (ddd, *J* = 8.1, 7.3, 1.4 Hz), 7.47 (ddd, *J* = 8.1, 1.6, 0.5 Hz)), 7.70 (1H, ddd, *J* = 7.8, 1.4, 0.5 Hz).

(2E)-3-(furan-2-yl)-1-(3-(1,2,3,6-tetrahydro-1-methylpyridin-4-yl)-2-hydroxy-4,6-dimethoxyphenyl)prop-2-en-1-one (JAPC6), $C_{21}H_{23}NO_5$, Orange crystalline, Molecular weight 369.41 UV: λ_{max} 334 nm (ε_{max} 42000), FT-IR υ'_{max} (cm^{-1}): 1631 (C=O) Mass (APCI +ve mode): m/z 370.16, $[M+1]^+$ ^1H NMR: δ 2.28-2.40 (5H, 2.28 (s), 2.34 (ddd, *J* = 15.0, 3.8, 2.0 Hz)), 2.72 (2H, ddd, *J* = 11.4, 10.1, 3.8 Hz), 3.09 (2H, dd, *J* = 13.9, 4.3 Hz), 3.85 (3H, s), 3.86 (3H, s), 5.98 (1H, dd, *J* = 4.3, 2.2 Hz), 6.19 (1H, s), 6.24 (1H, dd, *J* = 3.4, 2.6 Hz), 6.48-6.58 (2H, 6.56 (dd, *J* = 3.4, 1.0 Hz), 6.53 (d, *J* = 15.5 Hz)), 7.26 (1H, d, *J* = 15.5 Hz), 7.63 (1H, dd, *J* = 2.6, 1.0 Hz).

(2E)-3-(4-bromophenyl)-1-(3-(1,2,3,6-tetrahydro-1-methylpyridin-4-yl)-2-hydroxy-4,6-dimethoxyphenyl)prop-2-en-1-one(JAPC7), $C_{22}H_{22}BrNO_4$,Yellow Crystalline, Molecular weight 444.32, UV: λ_{max} 359 nm (ε_{max} 35000), FT-IR υ'_{max} (cm^{-1}): 1631 (C=O) (APCI +ve mode): m/z 446.07, $[M+2]^+$ ^1H NMR: δ 2.27-2.42 (5H, 2.28 (s), 2.34 (ddd, *J* = 15.0, 10.1, 3.8 Hz)), 2.72 (2H, ddd, *J* = 11.4, 10.1, 3.8 Hz), 3.08 (2H, dd, *J* = 13.9, 4.3 Hz), 3.85-3.87 (6H, 3.86 (s), 3.86 (s)), 5.98 (1H, dd, *J* = 4.3, 2.2 Hz), 6.12 (1H, s), 6.73 (1H, d, *J* = 15.7 Hz), 7.29-7.39 (2H, 7.35 (ddd, *J* = 8.1, 1.9, 1.7 Hz), 7.34 (ddd, *J* = 8.1, 8.0, 0.5 Hz)), 7.43 (1H, dt, *J* = 8.0, 1.7 Hz), 7.51 (1H, d, *J* = 15.7 Hz), 7.77 (1H, ddd, *J* = 1.9, 1.7, 0.5 Hz).

(2E)-1-(3-(1,2,3,6-tetrahydro-1-methylpyridin-4-yl)-2-hydroxy-4,6-dimethoxyphenyl)-3-(2-nitrophenyl)prop-2-en-1-one(JAPC8), $C_{23}H_{24}N_2O_6$, Brown crystalline, Molecular weight 424.45, UV: λ_{max} 324 nm (ε_{max} 19000), FT-IR υ'_{max} (cm^{-1}): 1631 (C=O) (APCI +ve mode): m/z 425.17, $[M+1]^+$ ^1H NMR: δ 2.28-2.40 (5H, 2.28 (s), 2.34 (ddd, *J* = 15.0, 3.8, 2.0 Hz)), 2.72 (2H, ddd, *J* = 11.4, 3.8, 2.0 Hz), 3.08 (2H, dd, *J* = 13.9, 4.3 Hz), 3.84 (3H, s), 3.86 (3H, s), 5.98 (1H, dd, *J* = 4.3, 2.2 Hz), 6.12 (1H, s), 6.99 (1H, d, *J* = 16.6 Hz), 7.86-8.00 (3H, 7.95 (d, *J* = 16.6 Hz), 7.89 (ddd, *J* = 8.3, 1.7, 0.5 Hz)), 8.12 (2H, ddd, *J* = 8.3, 1.9, 0.5 Hz).

(2E)-3-(3-bromophenyl)-1-(3-(1,2,3,6-tetrahydro-1-methylpyridin-4-yl)-2-hydroxy-4,6-dimethoxyphenyl)prop-2-en-1-one (JAPC9) $C_{23}H_{24}BrNO_4$, Yellow crystalline, Molecular weight 458.34, UV: λ_{max} 376 nm (ε_{max} 92000), FT-IR υ'_{max} (cm^{-1}): 1631 (C=O)

(APCI +ve mode): m/z 460.19, $[M+2]^+$ ^{1}H NMR: δ 2.28-2.40 (5H, 2.28 (s), 2.34 (ddd, *J* = 15.0, 3.8, 2.0 Hz)), 2.72 (2H, ddd, *J* = 11.4, 3.8, 2.0 Hz), 3.08 (2H, dd, *J* = 13.9, 4.3 Hz), 3.85-3.87 (6H, 3.86 (s), 3.86 (s)), 5.98 (1H, dd, *J* = 4.3, 2.2 Hz), 6.12 (1H, s), 6.73 (1H, d, *J* = 15.7 Hz), 7.29-7.39 (2H, 7.35 (ddd, *J* = 8.1, 1.9, 1.7 Hz), 7.34 (ddd, *J* = 8.1, 8.0, 0.5 Hz)), 7.43 (1H, dt, *J* = 8.0, 1.7 Hz), 7.51 (1H, d, *J* = 15.7 Hz), 7.77 (1H, ddd, *J* = 1.9, 1.7, 0.5 Hz).

(2E)-1-(3-(1,2,3,6-tetrahydro-1-methylpyridin-4-yl)-2-hydroxy-4,6-dimethoxyphenyl)-3-(4-methylthiophen-3-yl)prop-2-en-1-one(JAPC10) $C_{22}H_{25}NO_4S$**,** Light brown, Molecular weight 399.5, UV: λ_{max} 388 nm (ε_{max} 82000), FT-IR υ'_{max} (cm^{-1}): 1631 (C=O) (APCI +ve mode): m/z 400.15, $[M+1]^+$ ^{1}H NMR: δ 2.28-2.40 (5H, 2.28 (s), 2.34 (ddd, *J* = 15.0, 3.8, 2.0 Hz)), 2.35 (3H, s), 2.72 (2H, ddd, *J* = 11.4, 10.1, 3.8 Hz), 3.08 (2H, dd, *J* = 13.9, 4.3 Hz), 3.85-3.86 (6H, 3.86 (s), 3.86 (s)), 5.98 (1H, dd, *J* = 4.3, 2.2 Hz), 6.12 (1H, s), 6.80 (1H, d, *J* = 15.6 Hz), 7.03 (1H, d, *J* = 5.3 Hz), 7.35 (1H, d, *J* = 5.3 Hz), 7.50 (1H, d, *J* = 15.6 Hz). Physical characterization data of test compounds were presented in the Table 2.

Physico-chemical Characterization

Shake flask method was employed in the determination of lipophilicity of chalcones.[10] The compounds under investigation were solubilized in dimethyl sulphoxide followed by partitioning them into the biphasic system consisting of n-Octyl alcohol as organic phase and mono hydrogen phosphate buffer as aqueous phase which is presaturated at the pH of 7.4. The mixture was shaken for 24 h at 400 rpm and the lipophilicity was calculated as a ratio of the concentration of compound in aqueous phase to the concentration in the organic phase, which is expressed as LogD (distribution coefficient).

The redox potential of synthesized derivatives were measured using cyclic voltammetry utilizing Glassy carbon electrode as working electrode, silver-silver chloride as reference electrode and platinum wire as counter electrode. Test compounds and standard quercetin was dissolved in methanol and were added to the counter electrolyte solution (tetra butyl ammonium perchlorate) in the uniform concentrations and were scanned at 100 mVs^{-1}. The physico-chemical characterization data is presented in Table 2.

Table 2: Physico-chemical characterization for the synthesized test compounds.

Compound Code	Structure	Melting point (°C)	R_f value	% yield	Log D
NMC1	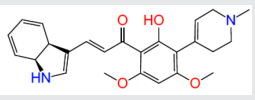	165	0.52	63	2.61
NMC2	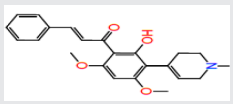	183	0.50	55	3.07
NMC3	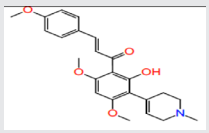	178	0.54	46	2.94
NMC4	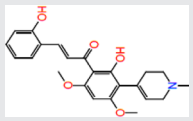	198	0.53	35	2.68
NMC5	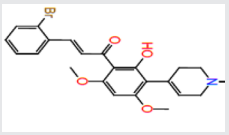	156	0.55	40	3.9
NMC6	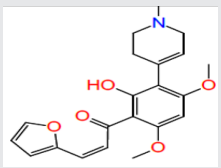	159	0.56	55	1.68
NMC7	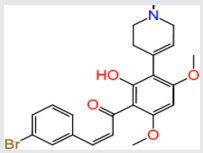	179	0.52	63	3.7
NMC8	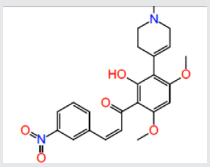	174	0.5	54	1.68
NMC9	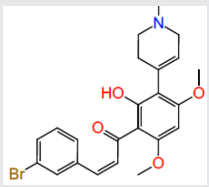	185	0.53	60	3.88
NMC10	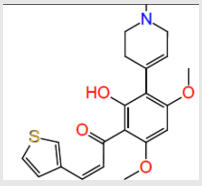	147	0.53	55	2.99

In vitro anti-oxidant and anticancer studies

DPPH Radical scavenging assay[11]

DPPH assay was carried out using the recommended protocols. In a 96 well plate, added 100µl of DPPH standard solution (concentration 200µM). The test

compounds were dissolved in methanol at varying concentrations and finally, added to the 96 well plates. The plate was incubated for 30 min and the absorbance was measured at 517 nm using an Elisa reader. The percentage inhibition is calculated as IC_{50} value.

ABTS radical scavenging assay[12]

ABTS free radical scavenging activity was performed according to the standard protocols. All the tests were carried out in a 96 well plate and final concentrations were prepared in methanol. ABTS reagent was prepared and kept overnight in the dark. The light green colored reagent was then added to the different concentrations of test samples. The absorbance was measured at 690nm and % inhibition is tabulated.

Nitric oxide radical scavenging (NO) assay

Nitric oxide free radical scavenging assay was carried out using Griess reaction reagent.[13] using 1.0 ml of 20 mM sodium nitroprusside as a nitrite donor in sodium hydrogen phosphate buffer mixed with specified amount of test samples at specified concentrations. The assay was carried out in 96 well plates, samples along with Griess reagent was incubated for 24 h at ambient temperature and absorbance was measured at 540 nm. The percentage inhibition was reported as IC_{50} value.

MTT assay[14]

MTT assay was performed to check the cytotoxic effect of chalcones on two cell lines. The cancer cells were grown in specified media (DMEM) consisting of 8-10 % phosphate buffered saline and 50 µg mL-1 erythromycin phosphate, maintained at ambient temperature with 5% CO_2. Specified number of cells were seeded in a 96-well plate and were incubated for a period of 24 h. Known concentration of sample solutions were prepared in DMSO. Quercetin was used as a standard drug. The absorbance was measured at 540 nm. The toxicity of the compounds on each cell lines were expressed as the IC_{50} value.

RESULTS AND DISCUSSION

Synthesis

2-hydroxychalcones substituted with N-methyl Piperidine (NMC 1–10) were synthesized following the standard procedure. Their chemical structures were confirmed by UV, IR, NMR and mass spectral analysis.

The UV spectrum of chalcones showed a principal maximum or k_{max} in the range of 320–390 nm[15] with e_{max} in the range of 3.4 $x10^3$–3.99x 104 cm^{-1} M^{-1}. The Fourier transform infrared spectrum showed a characteristic absorption peak in the range of 1604.77–1635.64 cm^{-1} which is assigned to the carbonyl carbon.[16] Furthermore, the NMR spectrum of the test compounds revealed structural features, namely a hydroxyl proton and protons of the alkenic double bonds. The hydroxyl proton showed a prominent singlet at 13.9 ppm and protons of the alkenic double bonds showed a double-doublet at 7.6-7.8. The final configuration of chalcones was assigned trans based on the J coupling values.

Anti-oxidant, anticancer and lipophilicity determination

Antioxidant studies

In the present study, anti-oxidant studies were performed for the synthesized chalcones (NMC1–10) also, the redox potential was determined using cyclic voltammeter. The results were interpreted using cyclic voltammograms. All the prepared chalcones showed an anodic peak corresponding to their oxidation potential or anodic potential (Epa) in the range of 0.422–0.658 V. Whereas, quercetin showed an antioxidant potential value of –0.691 V (Table 2). The synthesized compounds showed appreciable free radical scavenging effect by both DPPH and ABTS methods when compared to Nitric oxide method, as presented in Table 2. The ABTS radical scavenging activity of test compounds NMC5 (2-bromo derivative) and NMC10 (2-methyl thiophene derivative) with IC_{50} value of 61± 3.66 and 55.23 ± 2.87, respectively, was comparable to that of the standards in the IC_{50} range of 31.88± 5.87. Interestingly, amongst all the compounds tested, the compound NMC10 exhibited fairly a good antioxidant activity against ABTS radical which also showed lowest Epa of 0.480 V, supporting its *in-vitro* activity. The electron releasing resonance effect exerted by methoxy groups with a combination of hydroxyl group are important functional groups responsible for eliciting the antioxidant effects observed for the test compounds. Results of antioxidant studies were presented in the Table 3. Cyclic Voltammogram of one of the representative compound, NMC5 is given in the Figure 18.

In vitro anticancer activity

The anticancer activity for the test compounds were performed by MTT assay. The effect of test compounds on cell viability is expressed in terms of their IC_{50} value and were compared with a standard drug such as doxorubicin. as shown in the Table 3,[17] In the present study, chalcones NMC2 (benzaldehyde substituted), NMC5 (2-bromo derivative), NMC9 (3-bromomderivative)

Table 3: Results of anti-oxidant studies.				
Code	Radical scavenging activity, IC_{50} (Um)			Epa (V)# at 100 mV s^{-1}
	ABTS	DPPH	NITRIC OXIDE	
NMC1	77± 2.34	112± 4.88	>1000	0.539
NMC2	69±4.55	88±8.99	>1000	0.511
NMC3	117±8.55	134 ±5.77	957±21.56	0.626
NMC4	128±0.77	188 ±6.99	933± 33.45	0.649
NMC5	61± 3.66	85 ± 2.33	>1000	0.490
NMC6	156± 17.90	276 ±34.77	>1000	0.606
NMC7	85± 12.87	118±7.99	>1000	0.564
NMC8	112 ± 9.88	145 ± 8.88	>1000	------
NMC9	233±37.77	455 ±3.77	>1000	------
NMC10	55 ± 2.87	78 ±9.90	>1000	0.480
Quercetin	31.87 ±5.88	22±2.66	48±4.43	0.467

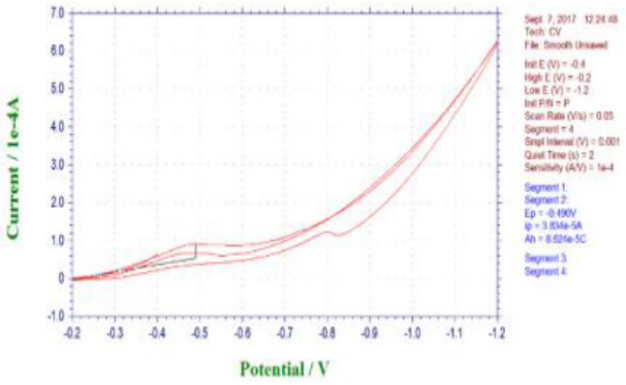

Figure 18: Cyclic Voltammogram for the most redox active compound NMC5.

and NMC10 (2-methyl thiophene derivative) have shown a significant cytotoxicity[18] against both MCF and Vero cell lines with an IC_{50} values of less than 25 micromolar which is comparatively better than that of the standard quercetin with an IC_{50} value of 102 and 26.2 micromolar against Vero and MCF cell lines. respectively. Anticancer activity of the synthesized test compounds are given in Table 4.

Determination of Lipophilicity

Lipophilicity[19] is one of the important experimental molecular descriptors, which helps in the determination of biological activity for drug candidates. In the present study, majority of the test compounds showed promising cytotoxicity, that possessed a log D values at the pH 7.4 values in the range between 2.4–4.2 as showed in Table 3.

CONCLUSION

In the present study, we have performed the anticancer screening for different N-methyl tetrahydropyridinyl substituted 2-hydroxychalcones against two cancer cell lines. Out of the 10 chalcones tested and evaluated, the chalcones namely, NMC2, NMC5, NMC9 and NMC10 emerged out as a potent antiproliferative agents with appreciable cytotoxicity against both MCF as well as VERO cell lines. The lipophilicity and redox potential were established. The present study provides an insight for the better understanding of mechanistic studies of N-methyl piperidinyl chalcones against anticancer targets such as both CDK and aromatase expressed in breast cancer cell lines

Table 4: Results of *in vitro* anticancer studies.			
S.NO.	NAME	IC_{50}-VERO (µM)	IC_{50}-MCF(µM)
	Quercetin (std)	>200	26.5
	NMC1	103.73	<25
	NMC2	<25	<25
	NMC3	83.33	48.12
	NMC4	100.82	128.29
	NMC5	<25	<25
	NMC6	>200	121.78
	NMC7	>200	>200
	NMC8	123.74	152.87
	NMC9	<25	<25
	NMC10	<25	<25

ACKNOWLEDGEMENT

Authors acknowledge Manipal Academy of Higher Education for the support provided, AICTE RPS for the support provided in carrying out Cyclic Voltammetric studies and Schrödinger Inc. USA for the software support provided to carry out molecular docking studies.

CONFLICT OF INTEREST

The authors declare no conflict of interest.

ABBREVIATIONS

CDK: Cyclin dependent Kinase; **ATP:** Adenosine triphosphate; **PDB:** Protein data bank; **NMR:** Nuclear magnetic resonance.

REFERENCES

1. Park E J, Park HR, Lee JS, Kim J. Licochalcone A: An Inducer of Cell Differentiation and Cytotoxic Agent from Pogostemon cabling1. Planta Medica. 1998;64(05):464-6.
2. Stoll R, Renner C, Hansen S, Palme S, Klein C, Belling A, *et al*. Chalcone derivatives antagonize interactions between the human oncoprotein MDM2 and p53. Biochemistry. 2001;40(2):336-44.
3. Lawrence NJ, McGown AT, Ducki S, Hadfield JA. The interaction of chalcones with tubulin. Anti-Cancer Drug Design. 2000;15(2):135-41.
4. Fu Y, Hsieh TC, Guo J, Kunicki J, Lee MY, Darzynkiewicz Z, *et al*. Licochalcone-A, a novel flavonoid isolated from licorice root (*Glycyrrhiza glabra*), causes G2 and late-G1 arrests in androgen-independent PC-3 prostate cancer cells. Biochemical and Biophysical Research Communications. 2004;322(1):263-70.
5. Edwards ML, Stemerick DM, Sunkara PS. Chalcones: A new class of antimitotic agents. Journal of Medicinal Chemistry. 1990;33(7):1948-54.
6. Ducki S, Forrest R, Hadfield JA, Kendall A, Lawrence NJ, McGown AT, *et al*. Potent antimitotic and cell growth inhibitory properties of substituted chalcones. Bioorganic and Medicinal Chemistry Letters. 1998;8(9):1051-6.
7. Bramson HN, Corona J, Davis ST, Dickerson SH, Edelstein M, Frye SV, *et al*. Oxindole-based inhibitors of Cyclin-Dependent Kinase 2 (CDK2): Design, synthesis, enzymatic activities and X-ray crystallographic analysis. Journal of Medicinal Chemistry. 2001;44(25):4339-58.
8. Schrödinger LLC. Schrödinger Release: LigPrep Version. New York, NY: Schrödinger, LLC. 2017. 2017;2.
9. Nigam S, Jayashree BS. Limitation of Algar-Flynn-Oyamada reaction using methoxy substituted chalcones as reactants and evaluation of the newly transformed aurones for their biological activities. Research on Chemical Intermediates. 2017;43(5):2839-64.
10. Ducki S, Forrest R, Hadfield JA, Kendall A, Lawrence NJ, McGown AT, *et al*. Potent antimitotic and cell growth inhibitory properties of substituted chalcones. Bioorganic and Medicinal Chemistry Letters. 1998;8(9):1051-6.
11. Blois MS. Antioxidant determinations by the use of a stable free radical. Nature. 1958;181(4617):1199.
12. Re R, Pellegrini N, Proteggente A, Pannala A, Yang M, Rice-Evans C. Antioxidant activity applying an improved ABTS radical cation decolorization assay. Free Radical Biology and Medicine. 1999;26(9-10):1231-7.
13. Green LC, Wagner DA, Glogowski J, Skipper PL, Wishnok JS, Tannenbaum SR. Analysis of nitrate, nitrite and [15N] nitrate in biological fluids. Analytical Biochemistry. 1982;126(1):131-8.
14. Denizot F, Lang R. Rapid colorimetric assay for cell growth and survival: Modifications to the tetrazolium dye procedure giving improved sensitivity and reliability. Journal of Immunological Methods. 1986;89(2):271-7.
15. Coxon CR, Anscombe E, Harnor SJ, Martin MP, Carbain B, Golding BT, *et al*. Cyclin-Dependent Kinase (CDK) inhibitors: Structure-activity relationships and insights into the CDK-2 selectivity of 6-substituted 2-arylaminopurines. Journal of Medicinal Chemistry. 2017;60(5):1746-67.
16. Sharma Y. Elementary Organic Spectroscopy Principle and Chemical Applications, Revised edn. S. Chand, New Delhi. 2015;114-22.
17. Elias DW, Beazely MA, Kandepu NM. Bioactivities of chalcones. Current Medicinal Chemistry. 1999;6(12):1125.
18. Monnier Y, Zaric J, Ruegg C. Inhibition of angiogenesis by non-steroidal anti-inflammatory drugs: From the bench to the bedside and back. Current Drug Targets-Inflammation and Allergy. 2005;4(1):31-8.
19. Jayashree BS, Patel HH, Mathew NS, Nayak Y. Synthesis of newer piperidinyl chalcones and their anticancer activity in human cancer cell lines. Research on Chemical Intermediates. 2016;42(4):3673-88.

SUMMARY

- Chalcones are one of the important class of compounds possessing a wide range of biological properties. One of the extensive area in research on chalcones is expressed in terms of their ability to act on various cancer cell lines by a variety of molecular mechanisms. Extensive literature search provided the information on methoxylated chalcones and their role in the inhibition of mitosis that could be further correlated to the structures of antimitotic agents like Combrestatin A and Colchicine possessing number of methoxy substituents. Chalcones processing methoxy groups, a trimethoxy substituted chalcone (PGHSD 234) is the most potent compound having cytotoxicity comparable to the standard drugs.
- A novel series of 10 piperidinyl chalcones were synthesized and characterized by physical and spectroscopic methods. The antioxidant and anticancer activity was determined. Also, molecular docking studies were performed to document their binding affinity towards the active site of CDK2/CyclinA.
- The MTT assay results showed the effect of various substituents on the chalcones template that could influence their cytotoxic effect. The hydrophobicity of the synthesized compounds were reported as distribution coefficient (Log D) and all the compounds showed LogD values in the range of 1.45–4.0. The cyclic voltammetry studies revealed their irreversible oxidation potential and were found to be in the range of -0.400 to -0.654.
- The present study provides an insight for the better understanding of mechanistic studies of N-methyl piperidinyl chalcones against anticancer targets such as both CDK and aromatase expressed in breast cancercell lines.

PICTORIAL ABSTRACT

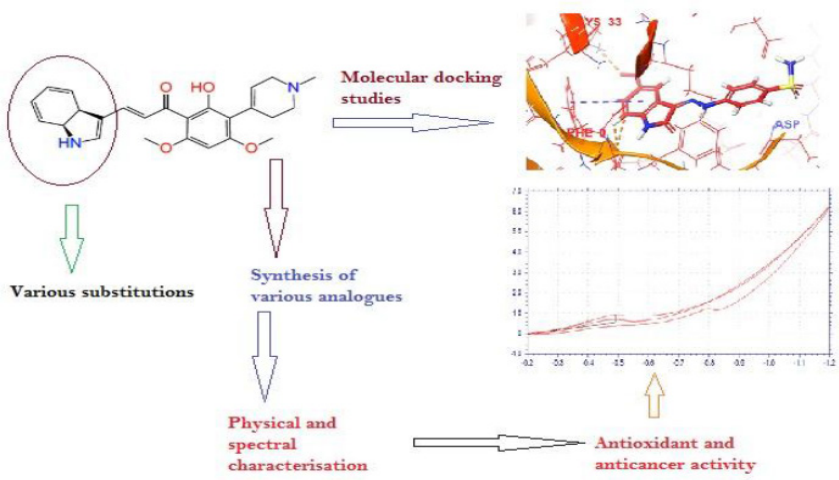

Cite this article: Pai A, Jayashree BS. Design, Synthesis and Biological Evaluation of Novel Piperidinyl Chalcones. Indian J of Pharmaceutical Education and Research. 2019;53(3 Suppl 2):s313-s324.